**Original papers**
***Materials for energy and environment, next-generation photovoltaics, and green technologies***

УДК 544.23.022.246 DOI: 10.17277/jamt-2025-10-03-200-214

# Structural features and properties of potassium polytitanates produced by $TiO_2$ powder processing in the molten nitrate-hydroxide mixtures of different composition

**© Natalia O. Morozova[a], Alexander V. Gorokhovsky[a]✉, Olga Yu. Grapenko[b]**

[a] *Yuri Gagarin State Technical University of Saratov, 77, Polytekhnicheskaya St., 410054, Saratov, Russian Federation,*
[b] *Research Institute of Physics, Southern Federal University,*
*194, Stachki Av., Rostov-on-Don, 344090, Russian Federation*

✉ algo54@mail.ru

**Abstract:** The paper studies the influence of the ratio of components in the $TiO_2$-KOH-$KNO_3$ reaction mixture on the structural properties of the quasi-amorphous particles of the product obtained (potassium polytitanate, PPT) which has the chemical composition of $K_2O{\cdot}(4.18 \pm 0.16)TiO_2{\cdot}(2.2 \pm 0.1)H_2O$. It is shown that by decreasing the KOH content in the melt used during heat treatment of $TiO_2$ powders (500 °C, 2 h), a degree of crystallinity of the PPT particles increases, while the proportion of the titanium in the valence state $Ti^{3+}$ and the amount of chemically adsorbed water decrease. The mechanism of the processes occurring during the synthesis of potassium polytitanate in nitrate- hydroxide melts is analyzed and an explanation for the patterns of change in the structure of the PPT particles observed with a change in the oxidizing properties of the meltis given. On the basis of the data obtained, some recommendations are given in order to use different variants of nitrate- hydroxide melts for the synthesis of PPT powders, depending on their further application.

**Keywords:** potassium titanates; synthesis; chemical composition; structure; defects; crystallinity; redox processes.

**For citation:** Morozova NO, Gorokhovsky AV, Grapenko OYu. Structural features and properties of potassium polytitanates produced by $TiO_2$ powder processing in the molten nitrate-hydroxide mixtures of different composition. *Journal of Advanced Materials and Technologies*. 2025;10(3):200-214. DOI: 10.17277/jamt-2025-10-03-200-214

# Структурные особенности и свойства полититанатов калия, полученных при обработке порошка $TiO_2$ в нитратно-гидроксидных расплавах различного состава

**© Н. О. Морозова[a], А. В. Гороховский [a]✉, О. Ю. Грапенко[b]**

[a] *Саратовский государственный технический университет имени Гагарина Ю. А.,*
*ул. Политехническя, 77, Саратов, 410054, Российская Федерация,*
[b] *Южный федеральный университет, Научно-исследовательский институт физики,*
*пр. Стачки, 194, Ростов-на-Дону, 344090, Российская Федерация*

✉ algo54@mail.ru

**Аннотация:** Исследовано влияние соотношения компонентов в реакционной смеси $TiO_2$-KOH-$KNO_3$ на структурные особенности квазиаморфных частиц полититаната калия (ПТК), имеющего химический состав $K_2O{\cdot}(4{,}18 \pm 0{,}16)TiO_2{\cdot}(2{,}2 \pm 0{,}1)H_2O$. С использованием методов просвечивающей и сканирующей микроскопии, рентгеновского фазового анализа, термического анализа, ИК-спектроскопии и рентгеновской фотоэлектронной микроскопии показано, что при снижении содержания KOH в расплаве, используемом при синтезе в ходе термической обработки порошков $TiO_2$ (500 °C, 2 ч), степень кристалличности структуры частиц ПТК увеличивается, доля титана в валентном состоянии $Ti^{3+}$, а также количество химически связанной воды – снижаются. Анализируется механизм процессов, протекающих при синтезе полититаната калия в нитратно-гидроксидных расплавах различного химического состава, и дается объяснение закономерностям в изменении

структуры частиц ПТК, наблюдаемым при изменении окислительной способности данных расплавов. На основании полученных данных даются рекомендации по использованию различных вариантов нитратно-гидроксидных расплавов для синтеза порошков ПТК в зависимости от их дальнейшего использования.

**Ключевые слова:** титанаты калия; синтез; химический состав; структура; дефекты; степень кристалличности; окислительно-восстановительные процессы.

**Для цитирования:** Morozova NO, Gorokhovsky AV, Grapenko OYu. Structural features and properties of potassium polytitanates produced by $TiO_2$ powder processing in the molten nitrate-hydroxide mixtures of different composition. *Journal of Advanced Materials and Technologies*. 2025;10(3):200-214. DOI: 10.17277/jamt-2025-10-03-200-214

## 1. Introduction

Quasiamorphous powders of potassium polytitanates (PPT) represent a new class of compounds that are currently used both as independent functional ceramic materials and composite fillers, and as intermediates for the synthesis of various functional products. A wide range of applications of PPT powders is associated with a number of their structural features and specific properties.

Regardless of the production method, potassium polytitanates consist of flaky particles of a layered structure similar to the crystalline structure of lepidocrocite, formed by double layers of titanium-oxygen octahedra [1–3], however, strongly distorted due to the presence of various defects (oxygen vacancies, the presence of titanium-oxygen octahedra in which titanium has different oxidation states, variation of the interlayer distance over a wide range, etc.). PPT particles have different degrees of hydration and variable chemical composition [4–7]). The $K^+$ cations located between the PPT layers and compensating for their negative charge are easily exchanged for $H_3O^+$ ions, which occurs already at the stage of washing the synthesized PPT powder to remove water-soluble components of the reaction mixtures used for its synthesis. As a result, the stoichiometric composition of PPT powders (molar ratio $n = [TiO_2]/[K_2O]$) can be changed within the range from 2 to 11 up to the complete removal of potassium due to treatment in water and aqueous acid solutions [8, 9].

Quasi-amorphous layered alkali metal polytitanates can be synthesized using various methods. In particular, this can be done using “soft chemistry” methods based on reactions in aqueous solutions at room temperature by exfoliating crystalline titanates with a layered structure, followed by restacking of nanosheets (polyanions) in solutions containing alkali metal cations [10]. The efficiency of such a synthesis method increases in the presence of various templates [11] or by applying an electrostatic field [12]. However, the synthesis methods of this group are complex multi-stage processes that involve the use of expensive technological equipment, and their use in large-scale production of the target product is problematic.

Hydrothermal treatment of titanium dioxide or metallic titanium powders in alkaline solutions at high pressures and at temperatures up to 200 °C [13] requires long reaction times and is often accompanied by the formation of crystalline titanates. In the case of using metallic titanium powder as a raw material, the process becomes technologically more complicated and the cost of the product increases significantly. It should be noted that hydrothermal synthesis of amorphous potassium polytitanates can also be carried out at atmospheric pressure [14] in the temperature range close to the boiling point of the alkaline solution. However, this is possible only in a very narrow temperature range, the random exit from which leads to the formation of crystalline potassium titanates. The use of complex methods combining the sol-gel and hydrothermal synthesis approaches, for example [15], encounters the same problems.

Synthesis of alkali metal titanates during processing in hydroxide-nitrate melts is the simplest technological method to implement, which allows organizing large-scale production of this product at relatively low production costs [9]. The theoretical basis for this synthesis is presented in [16]. It is based on the processing of $TiO_2$ powders in low-temperature melts based on $KNO_3$ or its mixtures with $K_2CO_3$ and/or KOH, followed by cooling the melt and removing water-soluble components of the raw material mixture and reaction by-products by washing with water or aqueous acid solutions.

Potassium polytitanates synthesized in nitrate-hydroxide melts are successfully used to obtain sorbents for extracting lithium from natural waters, as well as various pollutants from waste water, as solid electrolytes, antifriction materials and coatings, electrode and heat-reflecting materials, wear-resistant and high-strength polymer-matrix composites; ceramic materials with extremely high crack resistance, including special refractory ceramics, biocompatible ceramic implants, sensor elements of semiconductor sensors for analyzing gas environments, dielectrics, etc. [17–20]. Potassium

polytitanates modified in aqueous solutions of transition metal salts demonstrate excellent properties as highly effective photocatalysts active in the visible spectrum [21]. In addition, thermal treatment of both basic potassium polytitanate and PPT modified with transition metals can produce functional ceramics based on hollandite-like solid solutions, which have an abnormally high permittivity [22] in a wide temperature and frequency range.

Numerous areas of use and the formulation of the issue of developing an industrial large-scale production technology have revealed a number of problems associated with the fact that PPT powders synthesized in the $TiO_2$-$KNO_3$-KOH system with different component ratios exhibit different physicochemical and functional properties, despite the same chemical composition and quasi-amorphous structure. The same applies to products obtained on their basis during chemical and/or thermal treatment.

In this regard, the main objective of this study was to investigate the structural features of potassium polytitanate powders synthesized in the $TiO_2$-KOH-$KNO_3$ system under the same experimental conditions (temperature and synthesis time), differing only in the ratio of components, [KOH]/[$KNO_3$] and [$TiO_2$]/([KOH]+[$KNO_3$]). The aim of the work was to identify the conditions for the synthesis of PPT powders that ensure the production of products that provide their most effective use as specific types of functional materials or semi-finished products based on them.

## 2. Materials and Methods

### *2.1. Preparation of potassium polytitanate powders*

The synthesis of potassium polytitanate powders was carried out according to the standard method described in detail in [9] using $TiO_2$ (rutile, TU 2321-001-17547702-2014), KOH (Russian Standard 4363-80) and $KNO_3$ (Russian Standard R 53949-2010) as raw materials. After the preparation and homogenization of the raw material mixtures, the synthesis of PPT was carried out in an SNOL-1300 electric furnace in alundum ($Al_2O_3$) crucibles with heat treatment for 2 h (1 h heating at a rate of 10 °C·min$^{-1}$ and 1 h holding at 500 °C) followed by natural cooling of the crucible in the furnace with the power supply turned off. The composition of the raw material mixtures was varied in such a way as to obtain reaction mixtures with different ratios of components. The composition of the used raw mixtures is given in Table 1.

The KOH content in the reaction mixtures varied from 5 to 70 wt. %, and the $KNO_3$ content from 0 to 85 wt. %. In this case, the systems studied can be conditionally divided into 3 groups, characterized by different values of the ratio $x$ = [$TiO_2$]/([KOH] + + [$KNO_3$]), taking the values of 0.11; 0.25 and 0.43 (10, 20 and 30 wt. % $TiO_2$, respectively).

**Table 1.** Raw material mixtures used to produce potassium polytitanate

| PPT type | Raw material content and characteristics, wt.% | | | | | |
|---|---|---|---|---|---|---|
| | $TiO_2$ | KOH | $KNO_3$ | [$KNO_3$]/[KOH] ($x$) | [$TiO_2$]/[KOH] ($y$) | [$TiO_2$]/([KOH]+[$KNO_3$]) ($z$) |
| Group I | | | | | | |
| 30-70-0 | 30 | 70 | 0 | 0 | 0.43 | |
| 30-50-20 | 30 | 50 | 20 | 0.4 | 0.60 | 0.43 |
| 30-30-40 | 30 | 30 | 40 | 1.3 | 1.00 | |
| Group II | | | | | | |
| 20-53-27 | 20 | 53 | 27 | 0.5 | 0.38 | |
| 20-34-46 | 20 | 34 | 46 | 1.4 | 0.59 | 0.25 |
| 20-20-60 | 20 | 20 | 60 | 3.0 | 1.00 | |
| Group III | | | | | | |
| 10-77-13 | 10 | 77 | 13 | 0.2 | 0.13 | |
| 10-39-51 | 10 | 39 | 51 | 1.3 | 0.26 | |
| 10-30-60 | 10 | 30 | 60 | 2.0 | 1.0 | 0.11 |
| 10-10-80 | 10 | 10 | 80 | 8.0 | 1.0 | |
| 10-5-85 | 10 | 5 | 85 | 17.0 | 2.0 | |

The synthesized PPT powder was washed in a cycle that included two stages. At the first stage, the reaction mixture was pre-washed with distilled water (removal of residual water-soluble products and raw materials). The crucible with the reacted and cooled $TiO_2$-KOH-$KNO_3$ mixture (100 g by raw materials) was placed in a ceramic vessel with distilled water (1 L) and kept in it for 4 h (until the contents of the crucible were completely separated from the walls). The crucible was removed from the solution containing the obtained powder product and the dispersion was stirred using a propeller mixer-homogenizer (GZ120-S) for 1 hour. Then the obtained powder was separated from the solution using a high-speed centrifuge CF0201002 (4500 rpm) and used in the second stage of washing. At the second stage, washing was carried out sequentially with 0.4 L of water in portions with constant stirring for 2 h, followed by filtration through a paper filter (Whatman No. 42) and pouring in a new portion of water, after which the pH of the resulting aqueous dispersion was measured. In this case, 3 series of experiments were carried out with washing of products (PPT powders) that differed significantly in the composition of the raw material mixtures used for their synthesis. In particular, the products obtained in mixtures characterized by the ratios $[TiO_2] : [KOH] : [KNO_3]$ equal to 10 : 10 : 80, 20 : 20 : 60 and 30 : 30 : 40 at $x = [KNO_3]/[KOH] =$ 8.0; 3.0; 1.33 and $z = [TiO_2]/([KOH]+[KNO_3]) =$ 0.43; 0.25; 0.11, respectively.

At the end of each wash, the pH value of the obtained dispersion was determined using a pH meter (TAN-2). At the end of the full wash cycle, the obtained PPT powders were filtered, dried in a drying cabinet at a temperature of 50 °C (series A) for 4 h and subjected to high-energy milling in a Pulverizette 6 monoplanetary ball mill (series B).

The obtained dependence of the average (for five samples of each type of powder) pH value of aqueous dispersions after washing PPT with different amounts of water is shown in Fig. 1. The chemical composition of the product, measured by X-ray fluorescence analysis of PPT powders after a full cycle of washing, filtration and drying (50 °C/4 h), is also shown there.

The obtained results show that it is advisable to use 1.6 L of water to isolate potassium polytitanate powder (target product) from 100 g of the reacted $TiO_2$-KOH-$KNO_3$ reaction mixture, regardless of the mixture composition. Despite some differences in pH values with small portions of water, after using

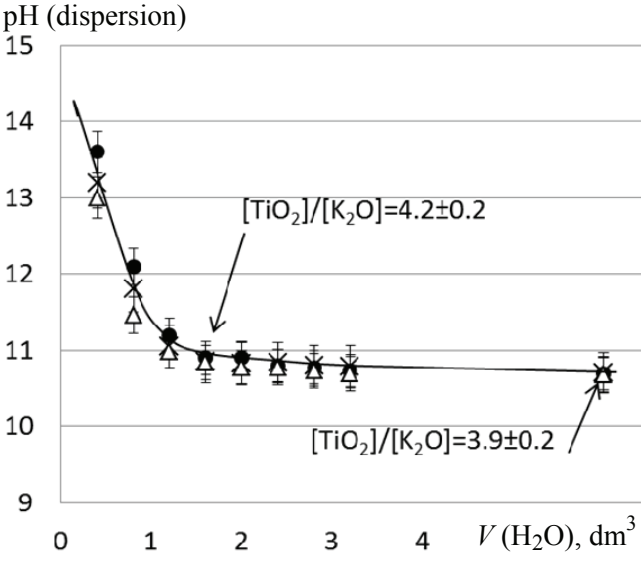


**Fig. 1.** pH values of the dispersion obtained by washing synthesized potassium polytitanate powders from residual KOH and $KNO_3$ using various quantities of distilled water with PPT (10-10-80) (Δ), PPT (20-20-60) (×) and PPT (30-30-40) (●). The curve shows a trend line. Systematic errors are given based on the results of measurements of 5 samples of each product type

four portions of 0.4 L, the hydrogen index of dispersion for all three types of powders had a close value (pH = 10.91 ± 0.15). At the same time, the chemical composition of the obtained PPT powders, after a full cycle of powder washing, filtration and drying, according to X-ray fluorescence analysis, was also approximately the same and corresponded to the molar ratio $[TiO_2]/[K_2O] = 4.18 \pm 0.16$.

During further washing (increasing the amount of water used), the pH of the aqueous dispersion decreased very slowly, reaching a pH of 10.70 ± 0.12 after washing with 6 L of water (control sample, see Fig. 1). But even in this case, the chemical composition of all the studied PPT powders changed insignificantly (up to $[TiO_2]/[K_2O] = 3.92 \pm 0.16$). A number of control experiments using other reaction mixtures of the studied system confirmed this conclusion.

The obtained results allow us to consider the potassium polytitanate powder obtained during synthesis (500 °C/2 h) in reaction mixtures of the $TiO_2$-KOH-$KNO_3$ system with different reagent ratios and washed with water according to the above method as a product of the same chemical composition with the possibility of comparing the structure and properties of its various types. The use of water for washing PPT powder in an amount

greater than 1.6 L per 100 g of the reacted reaction mixture is not advisable for economic reasons, since it has little effect on the chemical composition of the resulting product.

### *2.2. Analytic methods*

The characterization of PPT powders was carried out using transmission electron microscopy (TEM, JEOL JEM 1011 and Carl Zeiss Nvision 40), scanning electron microscopy (SEM, ASPEX, equipped with an energy dispersive analysis (EDS) attachment), X-ray phase analysis (ARL X'TRA), laser diffraction (Analysette 22 Microtec Plus), IR spectroscopy (FT-801) and X-ray photoelectron spectroscopy (XPS, VG Scientific ESCALAB). The thermal behavior of PPT powders was investigated using the DSC/TGA (NETZSCH STA 449 F3) equipment.

## 3. Results and Discussion

### *3.1. Particle morphology*

Particles of all types of PPT powders synthesized in nitrate-hydroxide melts of various compositions have a flaky shape (Fig. 2). According to TEM data, the size of these flakes varies from 10 to 60 nm and decreases regularly as the value of the parameter $x = [KNO_3]/[KOH]$ decreases and the value of the parameter $y = [TiO_2]/[KOH]$ increases in the melt used for synthesis.

An increase in the KOH content in the reaction mixture leads to a decrease in the size of the PPT particles. The TEM data also show that the flaky PPT particles are tactoids, i.e. anisotropic aggregates of nanosized particles (Fig. *3a*).

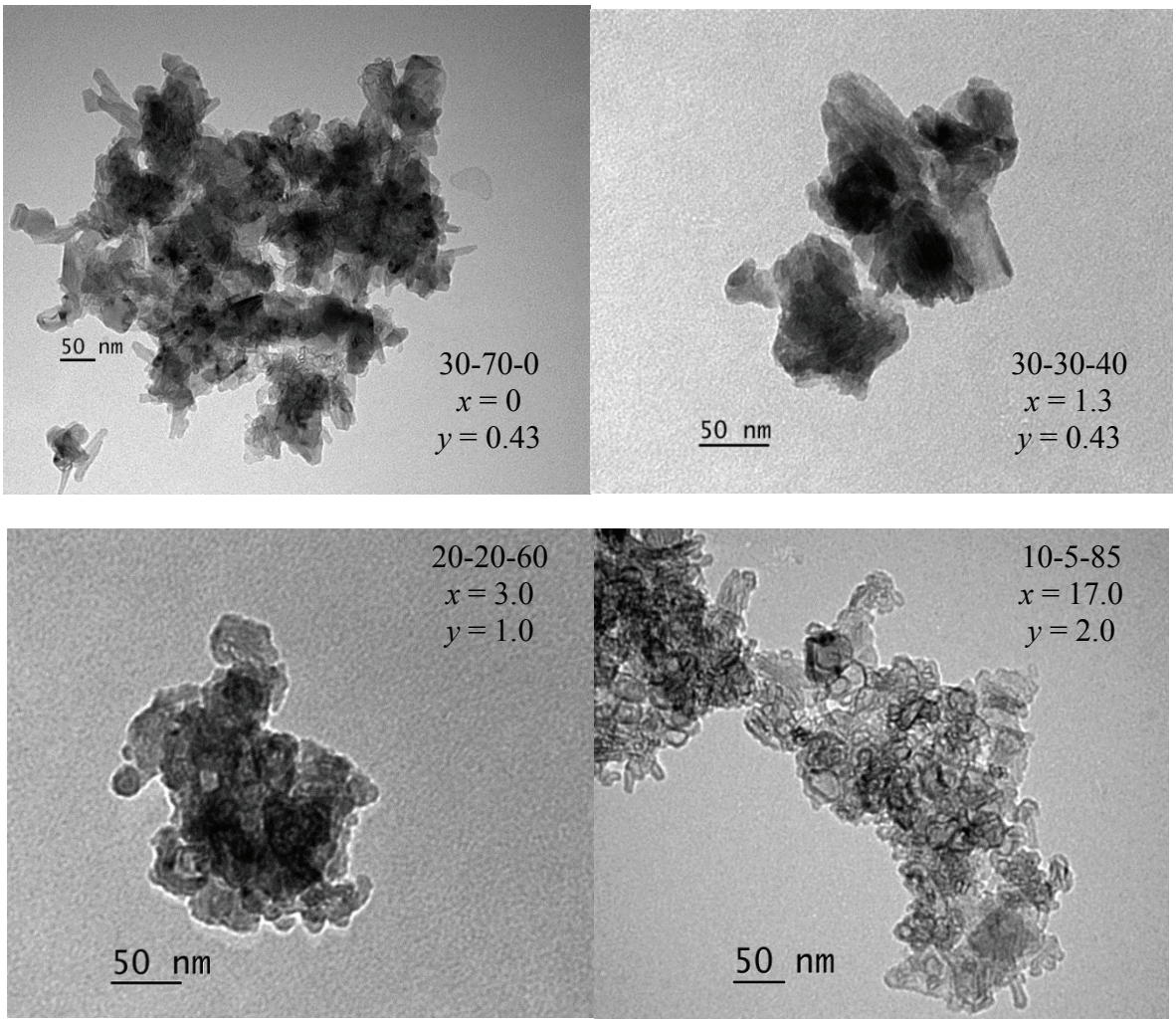


**Fig. 2.** TEM-images of agglomerated particles of PPT synthesized in different molten KOH-$KNO_3$ mixtures (compositions ate noted in accordance with Table 1)

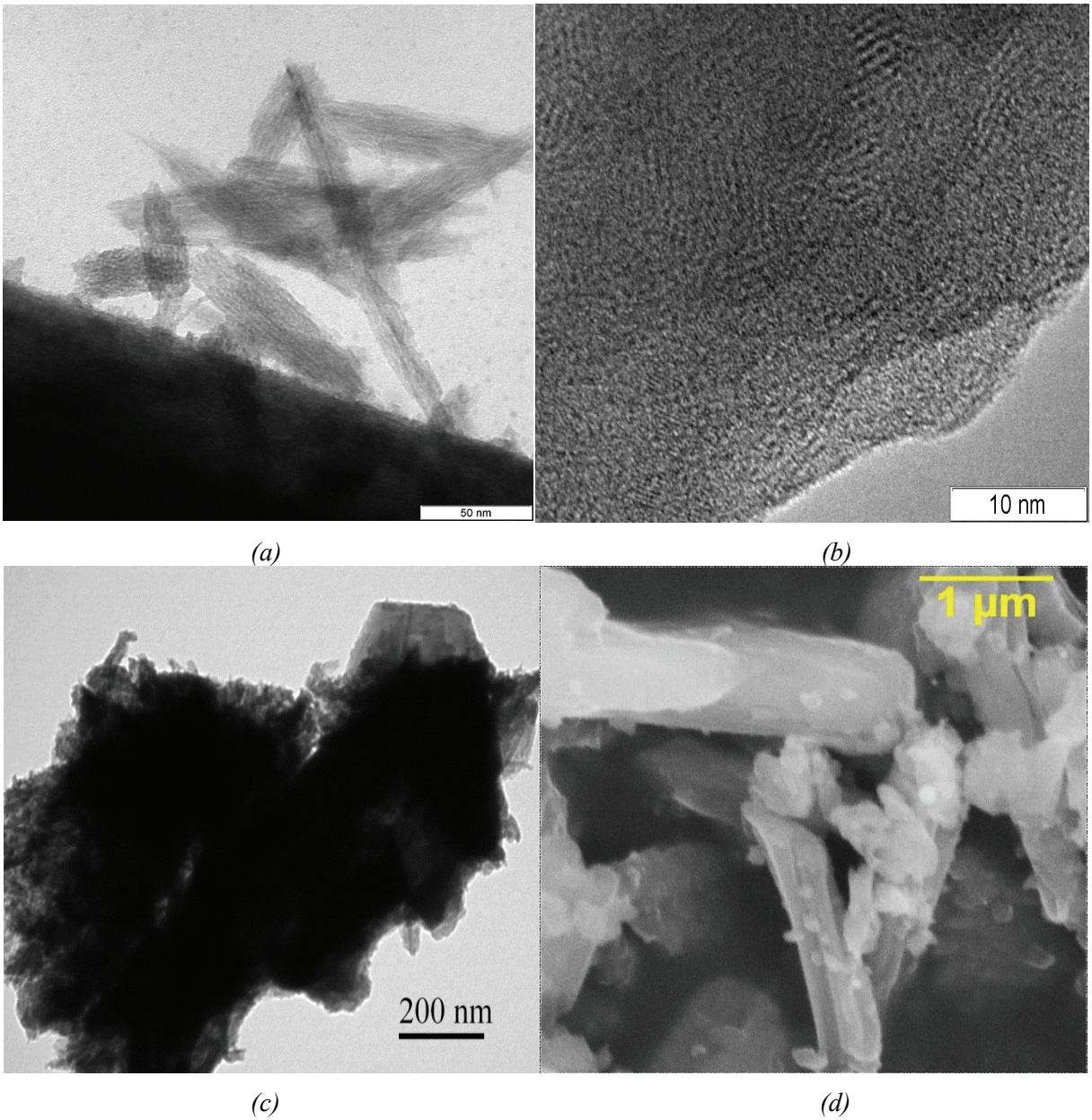


**Fig. 3.** Microphotographs of PPT particles and their agglomerates.
TEM of high resolution (*a* – composition 10-30-60; *b* – composition 30-30-40),
TEM (*c* – composition 20-20-60) and SEM (*d* – composition 10-30-60)

It can be stated that in the case of potassium polytitanate, such aggregates consist of domains with a more or less ordered structure, which are transformed into dispersed coagulation systems with a disordered structure (Fig. 3*b*, 3*c*). Typically, such a process occurs in sols during gelation [23], and during drying of the precipitates is accompanied by the phenomenon of syneresis. The precipitate obtained after washing the product synthesized in the reaction mixture with water, during drying, as a result of compaction of the spatial structural network of agglomerated PPT particles, can form aggregates of a fairly large size (up to 5 μm) (Fig. *3d*).

For all types of synthesized PPT, the use of the laser diffraction method after dispersion of dried powders in water and ultrasonic treatment allows us to obtain a distribution of its particles by size, characterized by the presence of three local maxima corresponding to agglomerates with an average size of about 0.1–0.2 and ~2 μm (Fig. 4). This distribution pattern for powders synthesized in various studied reaction mixtures differs somewhat quantitatively, but qualitatively coincides.

The analysis of the data presented in Fig. 4 allows us to conclude that, regardless of the composition of the reaction mixture used for

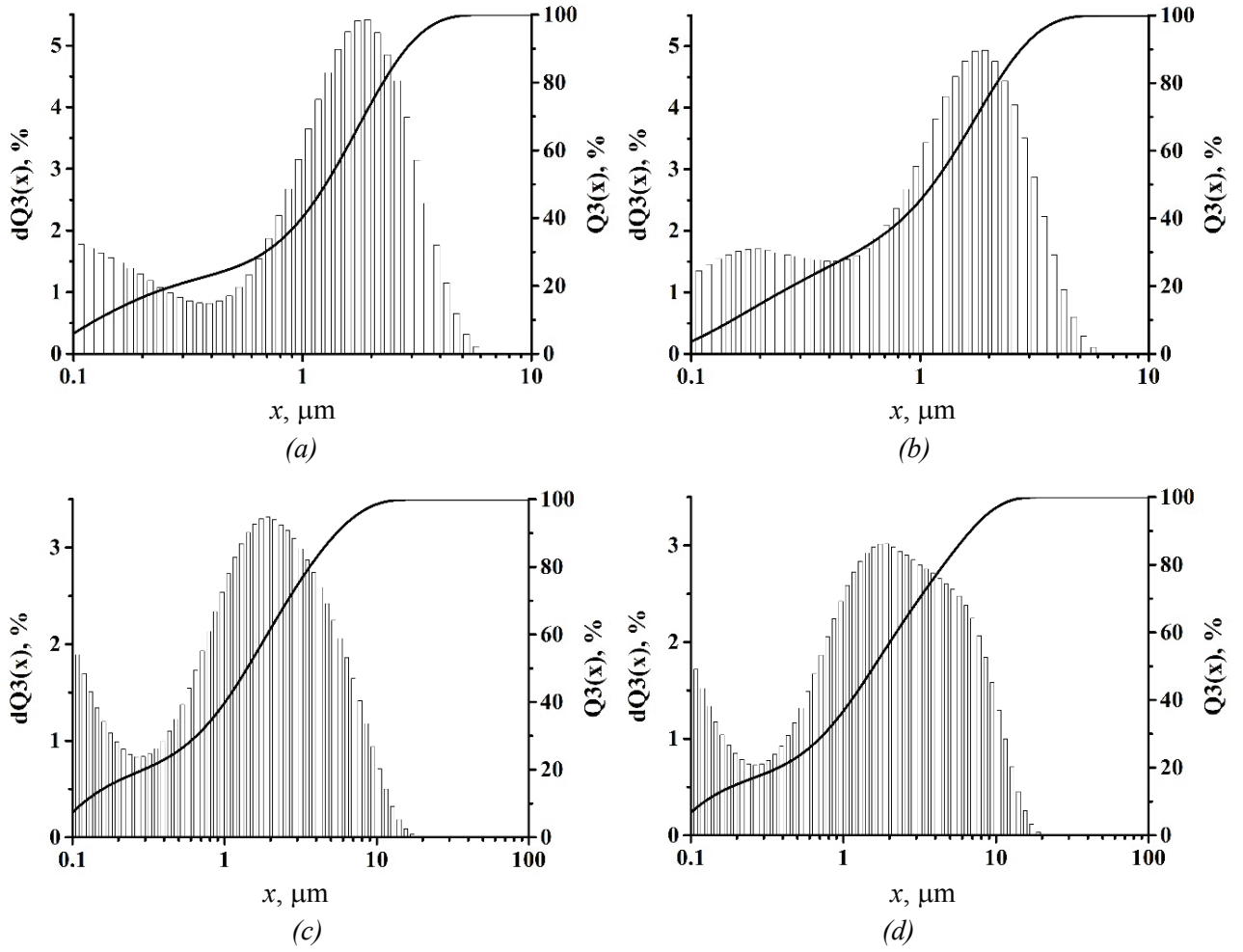


**Fig. 4.** Typical size distributions of particles in the aqueous dispersions obtained after the total washing cycle of PPT (30-30-40) (*a* and *c*) and PPT (30-70) (*b* and *d*) powders and additional dilution with $H_2O$ (1:9) (*a* and *b*), and the same produced with these powders after their filtration, drying (50 °C/2 h) and dilution with distilled water (*c* and *d*)

synthesis, the preparation of PPT powders should be carried out taking into account the direction of their further use. If it is preferable to use PPT powders in the form of submicron powders (production of antifriction or paint and varnish materials, nanocomposite catalysts and photoactive coatings, pharmacological agents, cosmetics), then it is advisable to use its aqueous dispersions obtained immediately after the last washing (to pH = = 10.91 ± 0.15) (Fig. 4*a*, 4*b*). If the particle size is not important, for example, in the production of ceramic materials and coatings, granulated sorbents, and also as raw materials for solid-phase synthesis of functional materials (hollandite-like and perovskite-like ferroelectrics), then it is possible to use dried powders in which PPT particles form fairly large microsized aggregates (Fig. 4*c*, 4*d*). In this case, drying is desirable to carry out at moderately high temperatures (40–50 °C), temperatures above 80 °C cause a sharp enlargement of the average size of PPT particle aggregates.

### *3.2. Degree of the structure orderliness*

The X-ray phase analysis data (Figs. 5 and 6) show that the degree of structure ordering (crystallinity) of potassium polytitanate powders synthesized in the $TiO_2$-KOH-$KNO_3$ system with different component ratios is different. As the $KNO_3$ content in the melt interacting with $TiO_2$ during the synthesis of PPT increases (increase in the value of the parameter $x$), the degree of crystallinity ($\alpha$) increases significantly from ~7 to ~20 %).

If potassium polytitanate was synthesized in melts characterized by $x = [KNO_3]/[KOH] < 0.5$, then the resulting powder can be considered quasi-amorphous ($\alpha < 10$ %), however, at $x > 2$, the resulting product is rather quasi-crystalline, since the content of the ordered crystalline phase in it reaches ~20 %. The analysis of X-ray diffraction patterns allows us to state that the structure of all types of PPT particles is close to the layered structure of crystalline

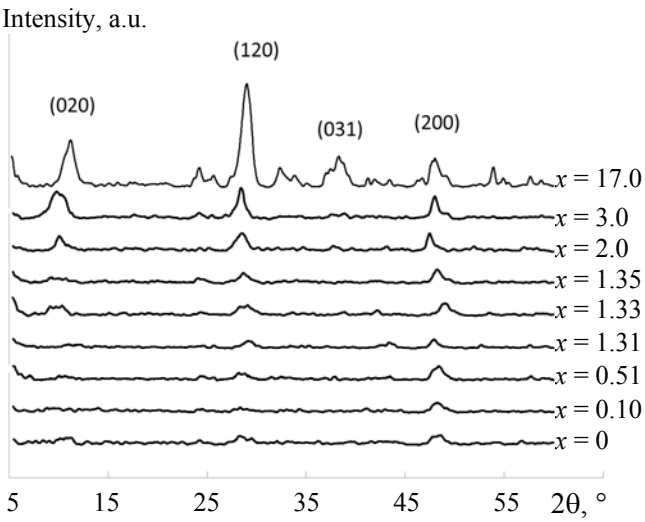


**Fig. 5.** XRD-patterns of PPT powders synthesized with different values of $x = [KNO_3]/[KOH]$

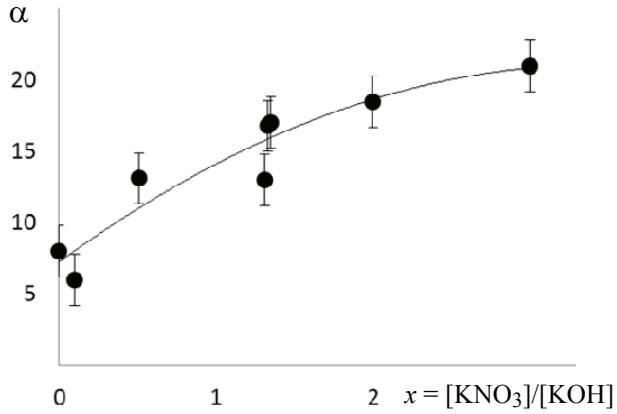


**Fig. 6.** Influence of $[KNO_3]/[KOH]$ ratio in the molten mixture on crystallinity (%) of the obtained PPT powder

lepidocrocite (database map JCPDF 75-2188), but is strongly distorted (see electronic photographs in Fig. *2a* and *2b*). In the case of PPT, reflections are quite clearly expressed at 2θ angles equal to 9,6° (020), 28.6° (120) and 47.9° (220) [24].

The reflex at an angle of 2θ ~ 37.9° (031) is practically not visible in most diffraction patterns and is very weakly expressed only in the PPT powder (10-5-85), which has a high degree of crystallinity and was obtained in a melt with a very high $KNO_3$ content.

If we talk about the degree of ordering of the lepidocrocite-like layered structure of PPT powder particles as a whole, then, according to the crystallographic characteristics, we can analyze the degree of ordering when considering various types of reflections in the X-ray diffraction patterns of PPT. The reflection at an angle of 2θ equal to 9.6° in the structure of crystalline potassium titanates is usually considered as a characteristic of the interlayer distance (020) [24]. In the X-ray diffraction patterns for PPT synthesized in melts at $x < 1.3$, this reflection is practically absent, which allows us to assert that in these types of PPT there is no ordering in the mutual arrangement of structural layers, and the interlayer distance varies within a fairly wide range. At the same time, for the reflection at an angle of 2θ equal to 47.8°, a well-defined reflection is present in the diffraction patterns of all types of PPT studied. This reflex is usually attributed to the mutual orientation of titanium-oxygen octahedra, which allows us to state that the mutual orientation of titanium-oxygen octahedra in the structure of individual layers of PPT is sufficiently stable and reproduced with a high degree of repeatability, regardless of the variation of the interlayer distance inside the PPT particles.

The size of the ordered regions in the structure of PPT particles obtained in melts characterized by $x > 1.3$, calculated using the Scherrer formula for all three observed reflexes, gives close values: 4.3–7.1 (reflex at 9.6°); 5.0–6.9 nm (reflex at 28.6°) and 3.6–5.1 (reflex at 47.9°), which, taking into account the high error in carrying out such calculations, allows us to estimate the crystallite size as 4–7 nm, regardless of the synthesis conditions. Therefore, in the lepidocrocite-like layered structure, such regions include regions of layers formed by 8–16 conjugated titanium-oxygen octahedra.

### *3.3. Water content and forms of its presence*

Thermal analysis methods were used to determine the content of various forms of water in the structure of various types of PPT. Typical DSC and TGA curves are shown in Fig. 7.

The TGA curves allow us to conclude that the powders of all studied types of PPT contain water released during heating. The total water content is 8–12 wt. %. At the same time, by analogy with our previous studies [9], three forms of water can be distinguished: physically sorbed, released in the temperature range of 100–250 °C; structural, present in the form of molecules located in the interlayer space of PPT particles and released in the temperature range of 250–500 °C; and chemically sorbed, present in the composition of thianol Ti-OH groups, decomposing with the release of molecular water at $T > 500$ °C (Fig. 7, Table 2). It is noteworthy that, depending on the conditions of synthesis of different types of PPT, the ratio of the amount of water presented in these three forms differs.

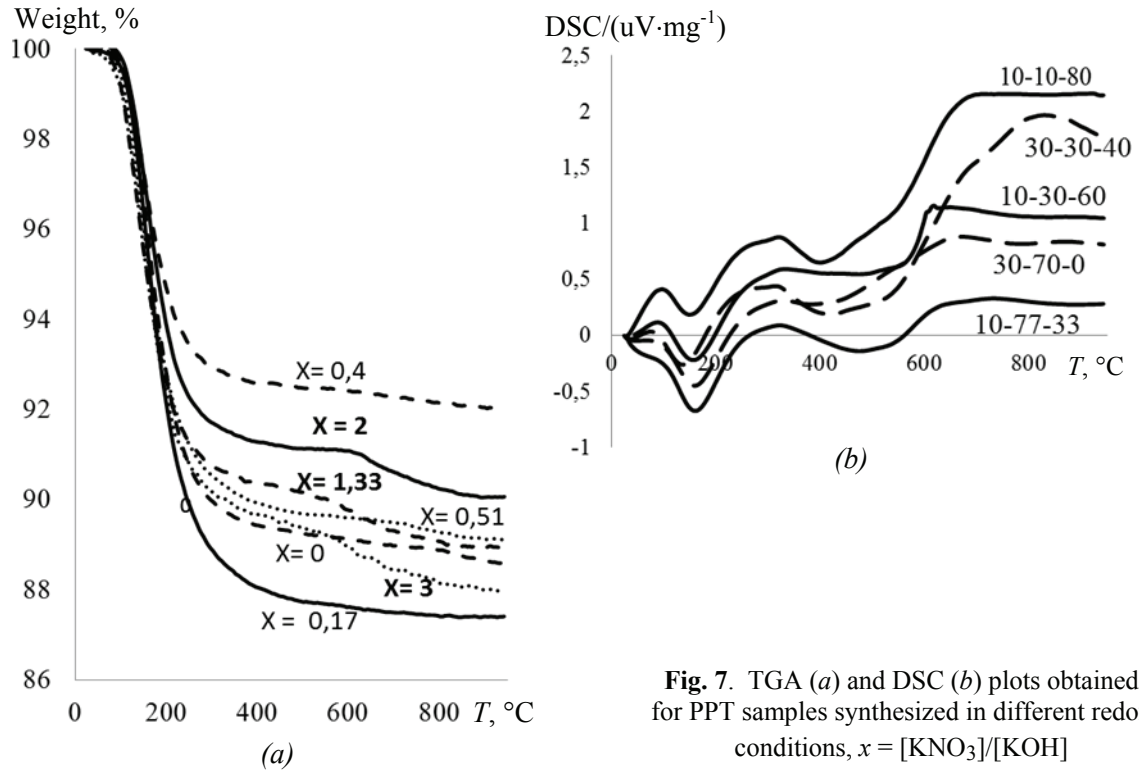


**Fig. 7**. TGA (*a*) and DSC (*b*) plots obtained for PPT samples synthesized in different redox conditions, $x = [KNO_3]/[KOH]$

**Table 2.** Content of various types of water in PPT powders produced in different experimental redox conditions (TGA data); $pH_{ie}$ – zero charge point (±0,1)

| $TiO_2$ : KOH : $KNO_3$ | $[KNO_3]/[KOH]$ ($x$) | $pH_{ie}$ | Water content, wt. % | | | | |
|---|---|---|---|---|---|---|---|
| | | | Physically adsorbed, 100–250 °C | Structural | | | Total |
| | | | | Interlayered, 250–500 °C | Chemically adsorbed, $T$ > 500 °C | Total structural | |
| 10-10-80 | **8** | 6.7 | 3.2 | 6.6 | **1.4** | **8.0** | **11.1** |
| 20-20-60 | **3** | – | 5.4 | 4.9 | **1.3** | **6.2** | 11.6 |
| 10-30-60 | **2** | 6.6 | 8.0 | 0.9 | **1.1** | **2.0** | 10.0 |
| 30-30-40 | **1.33** | 6.5 | 9.1 | 1.2 | **0.8** | **2.0** | 11.0 |
| 20-53-27 | 0.51 | – | 4.8 | 5.3 | 0.6 | 0.8 | 10.4 |
| 30-50-20 | 0.4 | 7.1 | 7.3 | 0.4 | 0.4 | 0.4 | 8.1 |
| 10-77-13 | 0.17 | – | 4.8 | 7.1 | 0.3 | 7.4 | 12.2 |
| 30-70 | 0 | 7.4 | 9.5 | 1.4 | 0.5 | 1.9 | 10.8 |

At the same time, structured water can be presented both in the form of molecules located between layers of individual polyanions that form scaly PPT particles, and between densely agglomerated individual scales.

Since the amount of physically adsorbed water depends on the average size of the agglomerates, it is quite difficult to draw detailed conclusions about the nature of the observed differences. However, it is noteworthy that the amount of chemically sorbed water ([TiOH] groups) is clearly tied to the value of $[KNO_3]/[KOH]$ in the reaction mixture used in the synthesis of PPT and regularly increases with the growth of the oxidizing capacity of the hydroxide-nitrate melt (increase in the value of $x = [KNO_3]/[KOH]$, Fig. 7).

Thus, the chemical activity of the surface of PPT particles, as well as the nature of their adhesive interactions associated with the presence of Brønsted acid centers, should differ significantly for different

types of PPT. This conclusion is confirmed by the results of the analysis of the IR absorption spectra obtained for PPT powders synthesized under different conditions (Fig. 8).

The study of the relative intensity of the absorption bands with maxima at 1630, 1558 and 1327 $cm^{-1}$, associated with angular vibrations of H-O-H in $H_2O$ molecules, $H_3O^+$ ions and Ti-O-H groups [25], shows that an increase in the value of the synthesis parameter $x = [KNO_3]/[KOH]$ leads to an increase in the content of water in the form of $H_3O^+$ and a decrease in the intensity of the absorption bands associated with the presence of molecular water in the composition of PPT, as well as thianol Ti-O-H groups.

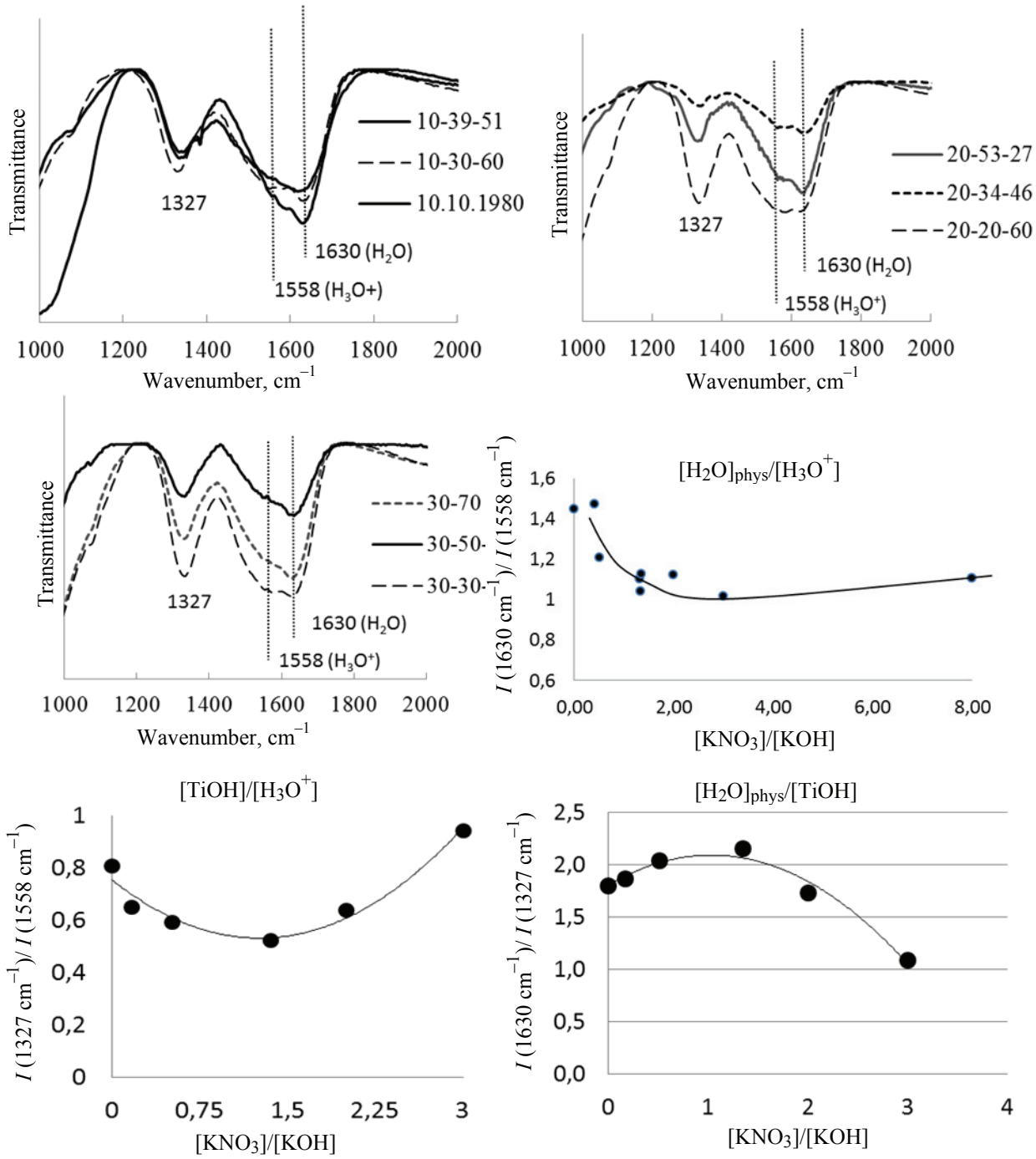


**Fig. 8.** IR-spectra of PPT powders produced with different $[KNO_3]/[KOH]$ in the molten mixture and dependence of the intensities for the absorption bands at 1630, 1558 and 1327 $cm^{-1}$, corresponding to δ (H-O-H) in $H_2O$ and $H_3O^+$, and Ti-O-H, respectively

This trend is also confirmed by the consideration of the relationship between the content of chemically sorbed water and the value of the point of zero charge of various PPT powders. It follows from the data in Table 2 that at $x = [KNO_3]/[KOH] > 1$, the value of the zero charge point, within the measurement error, has approximately one value ($6.6 \pm 0.2$), but with an increase in the oxidizing capacity of the melt (the value of $X$), it increases regularly, reaching a maximum value when using a single-component KOH melt ($7.2 \pm 0.1$). That is, the transition of the surface structure of PPT particles from the basic to the acidic type occurs at higher pH values. This directly indicates that at a low oxidizing capacity of the melt, the surface formed during synthesis has a higher content of Ti-O-H groups.

### *3.4. Presence of titanium in different valence states*

X-ray photoelectron spectroscopy (XPS; VG Scientific ESCALAB 250; AlKa, 15 kV, 20 mA) was used to estimate the Ti content in different valence states. All binding energy values (eV) were determined relative to the *C1s* line of carbon (285.0 eV) by the position of the peaks with an accuracy of ±0.2 eV.

The titanium content in different states in PPT powders synthesized in nitrate-hydroxide melts with different oxidizing capacity are given in Table 3.

PTT synthesized in a pure KOH melt contains the largest amount of $Ti^{3+}$ (21.9 at. % of the total titanium content) and even some amount of $Ti^{2+}$ (3.3 at. %). However, as $KNO_3$ is introduced into the melt, $[Ti^{2+}]$ in the PPT composition disappears, $[Ti^{3+}]$ naturally decreases to 10.6 at. %, and when using a melt with a very low KOH content ($[KNO_3]/[KOH] = 29$), titanium is present only in the valence state of $Ti^{4+}$.

**Table 3.** Contents of different forms of titanium in PPT powders produced in the molten mixtures with different $[KNO_3]/[KOH]$ ratios (XPS data)

| Characteristics of the chemical composition of the reaction mixture | | Proportion of titanium in different valence states (± 0.5 at. %) | | |
|---|---|---|---|---|
| $TiO_2 : KOH : KNO_3$ | $[KNO_3]/[KOH]$ | $Ti^{4+}$ | $Ti^{3+}$ | $Ti^{2+}$ |
| 30-70-0* | 0 | 74.8 | 21.9 | 3.3 |
| 30-50-20* | 0.4 | 83.9 | 16.1 | – |
| 20-20-60 | 3 | 86.5 | 13.5 | – |
| 10-10-80 | 8 | 89.4 | 10.6 | – |
| 10-5-85* | 29 | 100 | – | – |

* According to [4].

### *3.5. Mechanism of formation of the of PPT particle structure in melts with different oxidizing capacity*

The conducted studies showed that the structure of potassium polytitanate particles formed during the processing of $TiO_2$ powders in nitrate-hydroxide melts characterized by different ratios of $x = [KNO_3]/[KOH]$ (different oxidizing capacity) is significantly different. In particular, it can be stated that as the value of $x$ increases, the degree of hydration of the surface of PPT particles decreases (the concentration of Ti-OH groups decreases) and the content of $H_3O^+$ increases, with the same ratio of $[TiO_2]/[K_2O] = 4.18 \pm 0.16$. At the same time, an increase in the oxidizing capacity of the melt is accompanied by a decrease in the concentration of $Ti^{3+}$.

To explain the revealed patterns, it is necessary to consider the nature of the processes occurring at 500 °C in the $TiO_2$-KOH-$KNO_3$ system. It is known that the solubility of $TiO_2$ in media containing $OH^-$ ions increases significantly with an increase in $[OH^-]$ and temperature. In this case, alkali metal titanates with a layered structure ($M_2Ti_3O_7$) are formed as a solid phase [27, 28]

$$3TiO_2 + 2KOH = K_2Ti_3O_7\ (K_2Ti_4O_9) + H_2O.$$

A similar process can also occur in a $KNO_3$ melt

$$TiO_2 + 2KNO_3 \Rightarrow K_2TiO_3 + 2NO_2 + 1/2O_2\ ,$$

however, at $T < 550$ °C in the absence of hydroxide ions, this reaction is very slow [16].

The process of dissolution of titanium dioxide particles is accompanied by the transition of structural fragments of $TiO_2$ into the melt in the form of blocks of titanium-oxygen octahedra. The primary dissolution process occurs according to the reaction

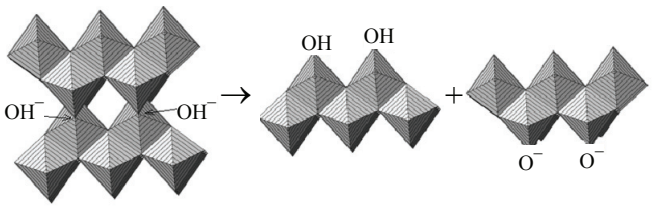


The structural fragments of $TiO_2$ that have passed into the melt are mainly presented in the form of various combinations of paired titanium-oxygen octahedra, which have a tendency to form layers due to the occurrence of a high-temperature polycondensation reaction [29], and the $K^+$ cations compensate for the excess negative charge of the layers (polyanions):

$$\{TiO_{6/2}\}_nTiO_{5/2}OH + HOTiO_{5/2}\{TiO_{6/2}\}_n + + mK^+ \rightarrow nH_2O +$$

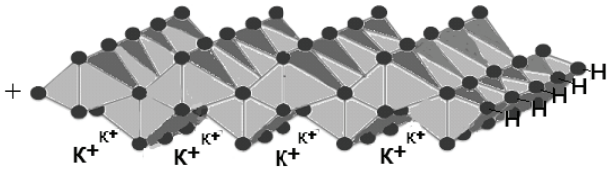


To explain the presence of trivalent titanium in various amounts in the structure of PPT particles, it should be noted that this effect is a fairly well-known phenomenon for both titanium dioxide and various titanates [30]. It is noted that the properties of the $TiO_2$ surface significantly depend on the presence of $Ti^{3+}$, which is considered as a defect in the crystal structure [31, 31]. It is noteworthy that the formation of defects in the form of $Ti^{3+}$ in titanium dioxide at temperatures above 450 °C occurs spontaneously [32]. In this case, the reduction of $Ti^{4+}$ to the $Ti^{3+}$ state can occur under the action of electrons, the source of which is $TiO_2$ itself. Thus, when $TiO_2$, which is a semiconductor, is heated to $T > 450$ °C, a thermally induced transition of an electron from the valence band to the conduction band occurs and an electron-hole pair ($e^-$, $h^+$) is formed in its structure [33]. $Ti^{4+}$ ions receive electrons from the oxygen of their own structure, and the oxygen itself can be removed from the crystal lattice with the formation of oxygen vacancies ($V_O$), which was previously confirmed by EPR data [34]

$$TiO_2\ (t°) \rightarrow e^- + h^+;$$

$$e^- + Ti^{4+} \rightarrow Ti^{3+};$$

$$4h^+ + 2O^{2-} \rightarrow O_2 + V_O{}^{2+}.$$

As a result, structural defects ($Ti^{3+}$, $V_O$) are formed, an important distinguishing feature of which is their high stability, especially in the absence of direct access to oxygen [35], and the ability to actively interact with the environment, acting as a reducing agent.

In melts with a very high content of $KNO_3$, the main anion is $NO_3^-$. As a result of its adsorption by the defective surface of structural blocks consisting of titanium-oxygen octahedra, the reaction occurs

$$Ti^{3+} + V_O{}^{2+} + NO_3^- \rightarrow Ti^{3+} + O^{2-} + NO_2^+ \rightarrow \rightarrow Ti^{4+} + O^{2-} + NO_2.$$

In this case, the nitrate ion sequentially decomposes according to the reaction

$$NO_3^- \rightarrow NO_2^+ + O^{2-},$$

which proceeds intensively at $T \sim 500$ °C [54], and the resulting $NO_2^+$ ion, in which nitrogen is in the valence state $N^{5+}$, oxidizes $Ti^{3+}$ to the state of $Ti^{4+}$, and itself passes into the state of $N^{4+}$ and is removed from the melt in the form of $NO_2$.

A similar action of nitrate ions was considered earlier [36]. As a result of the high oxidizing capacity of nitrate-hydroxide melts with a low KOH content, almost all thermally induced defects ($Ti^{3+}$, $V_O$) in the structure of the forming polytitanate polyanion are eliminated. Upon completion of the reaction, PPT particles contain a relatively small amount of titanium-oxygen octahedra $\{Ti^{3+}O_{6/2}\}$, which act as defects of the lepidocrocite-like crystal lattice, since their sizes differ from the octahedra $\{Ti^{4+}O_{6/2}\}$ [37]. The degree of ordering (crystallinity) of the PPT structure synthesized in melts with a high $KNO_3$ content is high (see Figs. 5 and 6). It should be noted that the oxidation-reduction processes on the surface of the Ti are in no way associated with the formation of Ti-O-H groups, which can explain their relatively low concentration in PPT powders synthesized in melts with high [$KNO_3$]/{KOH] values (see data in Tables 2 and 3).

However, as $KNO_3$ is replaced by KOH, the oxidizing ability of the melt decreases, since the $OH^-$ ions replacing $NO_3^-$ have a significantly lower reactivity when interacting with oxygen vacancies [36]. According to [38], $OH^-$ ions are capable of partially eliminating the above-mentioned thermally induced defects in the structure of titanate blocks ($Ti^{3+}$, $V_O$) due to the reaction

$$Ti^{3+}V_O + OH^- \rightarrow Ti^{4+}OH.$$

However, the rate of this reaction is low and in the absence of $NO_3^-$ ions in the melt, most of the $Ti^{3+}$ remains in a reduced state. As a result, the structure acquires a very high degree of defectiveness and becomes almost completely amorphous (Figs. 5 and 6).

In melts containing both $KNO_3$ and KOH, the reduction of $Ti^{3+}$ to $Ti^{4+}$ occurs via a mixed mechanism, and the contribution of $OH^-$ and $NO_3^-$ to the reduction process, as well as the degree of its completion, are determined by the ratio [$KNO_3$]/[KOH] in the melt used as a medium for the synthesis of PPT powders.

## 4. Conclusion

As a result of studying the conditions for synthesizing PPT powders during the processing of titanium dioxide in nitrate-hydroxide melts with

different [$KNO_3$]/[KOH] ratios, a number of patterns have been established. When using the same synthesis technique and the same chemical composition of the target product (PPT), the structural characteristics of the obtained powders, the morphology and fractional composition of their particles significantly depend on the [$KNO_3$]/[KOH] ratio in the reaction mixture used. It is noted that during synthesis in a melt with a low $KNO_3$ content, the lepidocrocite-like structure of the particles of the obtained product is characterized by a high degree of amorphization (degree of crystallinity less than 12 %), a high $Ti^{3+}$ content (more than 20 % of the total titanium content), a larger size of the agglomerates obtained during drying, and a higher content of chemically bound water (thianol groups).

As the $KNO_3$ content in the melt increases, accompanied by an increase in its oxidizing capacity, the structure of PPT particles becomes more and more ordered (the degree of crystallinity at the maximum $KNO_3$ content is 22 mol. %), the $Ti^{4+}$ content increases, reaching 100 %. At the same time, the average size of PPT particle agglomerates decreases. When using PPT powders for the production of thermal insulation materials and heat-reflecting coatings, as well as antifriction fillers for composite materials, the composition of the melt used for synthesis is not of fundamental importance, since the heat-reflecting and tribological characteristics of these powders do not depend on the degree of defectiveness of the PPT particle structure. When using PPT powders as photocatalysts for oxidation-reduction processes, biocidal additives, as well as photoactive components of photoelectron converters and precursor materials for the synthesis of complex titanates, it is advisable to select the composition of the melt during synthesis taking into account that the $Ti^{3+}$ content in the resulting product increases in direct proportion to the KOH content in the $KNO_3$-KOH mixture, reaching its maximum value when using a melt containing only KOH.

## 5. Funding

The study received financial support from the Foundation for Assistance to Small Innovative Enterprises (Project No. 23GTS2RES14/48796, TechnoStart Program).

## 6. Conflict of interest

The authors declare no conflict of interest.

## References

1. Sasaki T, Watanabe M, Michiue Y, Komatsu Y, et al. Preparation and acid-base properties of a protonated titanate with the lepidocrocite-like layer structure. *Chemistry of Materials*. 1995;7(5):1001-1007. DOI:10.1021/cm00053a029

2. Ma R, Bando Y, Sasaki T. Nanotubes of lepidocrocite titanates. *Chemical Physics Letters*. 2003;380(5-6):577-582. DOI:10.1016/j.cplett.2003.09.069

3. Maluangnont T, Arsa P, Limsakul K, Juntarachairot S, et al. Surface and interlayer base-characters in lepidocrocite titanate: the adsorption and intercalation of fatty acid. *Journal of Solid State Chemistry*. 2016;238:175-181. DOI:10.1016/j.jssc.2016.03.030

4. Gorokhovsky A, Morozova N, Yurkov G, Grapenko O, et al. Catalytic decomposition of $H_2O_2$ in the aqueous dispersions of the potassium polytitanates produced in different conditions of molten salt synthesis. *Molecules.* 2023;28(13):4945. DOI:10.3390/molecules 28134945

5. Pei Q, He T, Yu Y, Jing Z, et al. Fabrication of oxygen vacancies through assembling an amorphous titanate overlayer on titanium oxide for a catalytic water–gas shift reaction. *Journal of Materials Chemistry A.* 2021;9(5):2784-2791. DOI:10.1039/D0TA11641F

6. Kitano M, Wada E, Nakajima K, Hayashi S, et al. Protonated titanate nanotubes with Lewis and Brønsted acidity: relationship between nanotube structure and catalytic activity. *Chemistry of Materials*. 2013;25(3):385-393. DOI:10.1021/cm303324b

7. Riss A, Berger T, Grothe H, Bernardi J, Diwald O, Kno1zinger E. Chemical control of photoexcited states in titanate nanostructures. *Nano Letters.* 2007;7(2):433-438. DOI:10.1021/nl062699y

8. Zhang S, Chen Q, Peng L-M. Structure and formation of $H_2Ti_3O_7$ nanotubes in an alkali environment. *Physical Review B.* 2005;71(1):014104. DOI:10.1103/ PhysRevB.71.014104

9. Sanchez-Monjaras T, Gorokhovsky AV, Escalante-Garcia JI. Molten salt synthesis and characterization of polytitanate ceramic precursors with varied $TiO_2/K_2O$ molar ratio. *Journal of the American Ceramic Society*. 2008;91(9):3058-3065. DOI:10.1111/ j.1551-2916.2008.02574.x

10. Liu T, Miao L, Yao F, Zhang W, et al. Structure, properties, preparation, and application of layered titanates. *Inorganic Chemistry.* 2024;63(1):1-26. DOI:10.1021/ acs.inorgchem.3c03075

11. Mastoroudes BC, Markgraaff J, Wagener JB, Olivier EJ. Synthesis of cesium, sodium and nitrogen derived titanates using the Pechini sol-gel method. *Chemical Physics.*2020;537:110816. DOI:10.1016/ j.chemphys.2020.110816

12. Xu L, Pan C, Li S, Yin C, et al. Electrostatic self-assembly synthesis of three-dimensional mesoporous lepidocrocite-type layered sodium titanate as a superior adsorbent for selective removal of cationic dyes via an ion-

exchange mechanism. *Langmuir*. 2021;37(19):6080-6095. DOI:10.1021/acs.langmuir.1c00913

13. Hayashi H, Hakuta Y. Hydrothermal synthesis of metal oxide nanoparticles in supercritical water. *Materials*. 2010;3:3794-3817. DOI:10.3390/ma3073794

14. Liu Y, Qi T, Zhang Y. A novel way to synthesize potassium titanates. *Materials Letters*. 2006;60(2):203-205. DOI:10.1016/j.matlet.2005.08.017

15. Zima T, Baklanova N, Bataev I. Synthesis and characterization of hybrid nanostructures produced in the presence of the titanium dioxide and bioactive organic substances by hydrothermal method. *Journal of Solid State Chemistry*.2012;198:131-137. DOI:10.1016/j.jssc.2012.09.019

16. Afanasiev P. Molten salt syntheses of alkali metal titanates. *Journal of Materials Science*. 2006;41(4):1187-1195. DOI:10.1007/s10853-005-3656-2

17. Vikulova MA, Maksimova LA, RudyhVYu, Gorshkov NV. Selective lithium extraction from aqueous solutions by layered amorphous protonated potassium polytitanate. *Journal of Advanced Materials and Technologies*. 2023;8(1):60-69. DOI:10.17277/jamt.2023.01.pp.060-069

18. Fedorov FS, Varezhnikov AS, Kiselev I, Kolesnichenko VV, et al. Potassium polytitanate gas-sensor study by impedance spectroscopy. *Analytica Chimica Acta*. 2015;897:81-86. DOI:10.1016/j.aca.2015.09.029

19. Goffman VG, Gorokhovsky AV, Kompan MM, Tretyachenko EV, et al. Electrical properties of the potassium polytitanate compacts. *Journal of Alloys and Compounds*. 2014;615:526-529. DOI:10.1016/j.jallcom.2014.01.121

20. Gorokhovsky AV, Tsiganov AR, Nikityuk TV, Escalante-Garcia JI, et al. Synthesis and properties of nanocomposites in the system of potassium polytitanate-layered double hydroxide. *Journal of Materials Research and Technology*. 2020;9(3):3924-3934. DOI:10.1016/j.jmrt.2020.02.018

21. Tretyachenko EV, Gorokhovsky AV, Yurkov GY, Fedorov FS., et al. Adsorption and photo-catalytic properties of layered lepidocrocite-like quasi-amorphous compounds based on modified potassium polytitanates. *Particuology*. 2014;17:22-28. DOI:10.1016/j.partic.2013.12.002

22. Shirpour M, Cabana J, Doeff M. Lepidocrocite-type layered titanate structures: new lithium and sodium ion intercalation anode materials. *Chemistry of Materials*. 2014;26(8):2502-2512. DOI:10.1021/cm500342m

23. Xu Z, Wang L, Fang F, Fu Y, Yin Z. A review on colloidal self-assembly and their applications. *Current Nanoscience*. 2016;12(6):725-746. DOI:10.2174/1573413712666160530120807

24. Xu J, Zhang H, Zhang J, Liu X, He X, Xu D, Sun J. Hydrothermal synthesis of potassium/sodium titanate nanofibres and their ultraviolet properties. *Micro & Nano Letters*. 2012;7(5):407-411. DOI:10.1049/mnl.2012.0116

25. Timokhin VM, Garmash VM, Tedzhetov VA. Spectral diagnostics of oscillation centers in crystals with hydrogen bonds. *Izvestiya Vysshikh Uchebnykh Zavedenii. Materialy Elektronnoi Tekhniki = Materials of Electronics Engineering*. 2019;5(2):61-68. DOI:10.17073/1609-3577-2019-1-35-44 (In Russ.)

26. Panayotov DA, Yates Jr JT. Depletion of conduction band electrons in $TiO_2$ by water chemisorptions-IR spectroscopic studies of the independence of Ti-OH frequencies on electron concentration. *Chemical Physics Letters*. 2005;410(1-3):11-17. DOI:10.1016/j.cplett.2005.03.146

27. Shkol′nikov YeV. Effect of polymorphism and dispersion of titanium dioxide on solubility in acidic and alkaline media. *Izvestiya Sankt-Peterburgskoy lesotekhnicheskoy akademii*. 2016;215:266-275. (In Russ.)

28. Sampath AJ, Wickramasinghe ND, de Silva KN, de Silva RM. Methods of extracting $TiO_2$ and other related compounds from Ilmenite. *Minerals*. 2023;13(5):662. DOI:10.3390/min13050662

29. Tominaka S, Yamada H, Hiroi S, Kawaguchi SI, Ohara K. Lepidocrocite-type titanate formation from isostructural prestructures under hydrothermal reactions: observation by synchrotron X-ray total scattering analyses. *ACS Omega*. 2018;3(8):8874-8881. DOI:10.1021/acsomega.8b01693

30. Diebold U, Lehman J, Mahmoud T. Intrinsic defects on a $TiO_2(110)(1 \times 1)$ surface and their reaction with oxygen: a scanning tunneling microscopy study. *Surface Science*. 1998;411(1-2):137-153. DOI:10.1016/S0039-6028(98)00356-2

31. Henrich VE, Kurtz RL. Surface electronic structure of $TiO_2$: atomic geometry, ligand coordination, and the effect of adsorbed hydrogen. *Physical Review B*. 1981;23(12):6280-6287. DOI:10.1103/PhysRevB.23.6280

32. Lu G, Linsebigler A, Yates JT. $Ti^{3+}$ defect sites on $TiO_2(110)$: production and chemical detection of active sites. *Journal of Physical Chemistry*. 1994;98(45):11733-11738. DOI:10.1021/j100096a017

33. Xiong LB, Li JL, Yang B, Yu Y. $Ti^{3+}$ in the surface of titanium dioxide: generation, properties and photocatalytic application. *Journal of Nanomaterials*. 2012;2012(1):831524. DOI:10.1155/2012/831524

34. Raupp GB, Dumesic JA. Adsorption of CO, $CO_2$, $H_2$, and $H_2O$ on titania surfaces with different oxidation states. *The Journal of Physical Chemistry*. 1985;89(24):5240-5246. DOI:10.1021/j100270a024

35. Sirisuk A, Klansorn E, Praserthdam P. Effects of reaction medium and crystallite size on $Ti^{3+}$ surface defects in titanium dioxide nanoparticles prepared by solvothermal method. *Catalysis Communications*. 2008;9(9):1810-1814. DOI:10.1016/j.catcom.2008.01.035

36. Parrino F, Livraghi S, Giamello E, Ceccato R, Palmisano L. Role of hydroxyl, superoxide, and nitrate radicals on the fate of bromide ions in photocatalytic $TiO_2$ suspensions. *ACS Catalysis*. 2020;10(14):7922-7931. DOI:10.1021/acscatal.0c02010

37. Stoyanov E, Langenhorst F, Steinle-Neumann G. The effect of valence state and site geometry on $TiL_{3,2}$ and OK electron energy-loss spectra of $Ti_xO_y$ phases. *American Mineralogist.* 2007;92(4):577-586. DOI:10.2138/am.2007.2344

38. Lu TC, Wu YS, Lin LB, Zheng WC. Defects in the reduced rutile single crystal. *Physica B: Condensed Matter.* 2001;304(1-4):147-151. DOI:10.1016/S0921-4526(01)00337-4

## Information about the authors / Информация об авторах

**Natalia O. Morozova,** Laboratory Researcher, Yuri Gagarin State Technical University of Saratov (SSTU), Saratov, Russian Federation; ORCID 0000-0002-1470-0011; e-mail: DLG2@yandex.ru

**Alexander V. Gorokhovsky,** D. Sc. (Chem.), Professor, Head of the Department, SSTU, Saratov, Russian Federation; ORCID 0000-0002-4210-3169; e-mail: algo54@mail.ru

**Olga Yu. Grapenko,** Junior Researcher, Research Institute of Physics, Southern Federal University, Rostov-on-Don, Russian Federation; ORCID 0000-0001-5749-1515; e-mail: grapenko@sfedu.ru

**Морозова Наталья Олеговна,** лаборант-исследователь, Саратовский государственный технический университет имени Гагарина Ю. А. (СГТУ имени Гагарина Ю.А.), Саратов, Российская Федерация; ORCID 0000-0002-1470-0011; e-mail: DLG2@yandex.ru

**Гороховский Александр Владиленович,** доктор химических наук, профессор, заведующий кафедрой, СГТУ имени Гагарина Ю.А., Саратов, Российская Федерация; ORCID 0000-0002-4210-3169; e-mail: algo54@mail.ru

**Грапенко Ольга Юрьевна,** младший научный сотрудник, Южный федеральный университет, Научно-исследовательский институт физики, Ростов-на-Дону, Российская Федерация; ORCID 0000-0001-5749-1515; e-mail: grapenko@sfedu.ru

*Received 05 March 2025; Revised 31 March 2025; Accepted 08 April 2025*